| 1 | The importance of climate and anthropogenic influence in precipitation partitioning |
|----|---|
| 2 | in the contiguous United States |
| 3 | |
| 4 | Sara Alonso Vicario ^a , George M. Hornberger ^b , Maurizio Mazzoleni ^c , and Margaret |
| 5 | Garcia ^a |
| 6 | |
| 7 | ^a School of Sustainable Engineering & the Built Environment, Arizona State University, Tempe, |
| 8 | Arizona, USA |
| 9 | ^b Department of Civil and Environmental Engineering, Vanderbilt University, Nashville, |
| 10 | Tennessee, USA |
| 11 | ^c Institute for Environmental Studies, Vrije Universiteit Amsterdam, Amsterdam, The |
| 12 | Netherlands |
| 13 | Corresponding author: Sara Alonso Vicario (<u>saralonsovicario@gmail.com</u>). Postal address: |
| 14 | Walton Center For Planetary Health 777 E University Dr, Tempe, AZ 85287, USA |
| 15 | |
| 16 | |
| 17 | |

Abstract

18

19

20

21

22

23

24

25

26

27

28

29

30

31

32

33

34

35

36

37

38

39

Understanding the process of precipitation partitioning into evapotranspiration and streamflow is fundamental for water resource planning. The Budyko framework has been widely used to evaluate the factors influencing this process. Still, its application has primarily focused on studying watersheds with minimal human influence and on a relatively small number of factors. Furthermore, there are discrepancies in the literature regarding the effects of climatic factors and land use changes on this process. To address these gaps, this study aims to quantify the influence of climate and anthropogenic activities on streamflow generation in the contiguous United States. To accomplish this, we calibrated an analytical form of the Budyko curve from 1990 to 2020 for 383 watersheds. We developed regional models of ω , a free parameter introduced to account for controls of precipitation partitioning not captured in the original Budyko equation, within different climate zones. We computed 49 climatic and landscape factors that were related to ω using correlation analysis and stepwise multiple linear regression. The findings of this study show that human activities explained a low variance of the spatial heterogeneity of ω compared with the watershed slope and the synchronization between precipitation and potential evapotranspiration, nevertheless, urban development emerged as a factor in temperate climates, whereas irrigated agriculture emerged in cold climates. In arid climates, mean annual precipitation explains less than 20% of the spatial variability in mean annual streamflow; furthermore, this climate is the most responsive to changes in ω . These results provide valuable insights into how land use and climate interact to impact streamflow generation differently in the contiguous United States contingent on the regional climate, explaining discrepancies in the literature.

Keywords: Budyko, Streamflow, Land use, Climate zones, Stepwise multiple linear regression

1 Introduction

40

41

42

43

44

45

46

47

48

49

50

51

52

53

54

55

56

57

58

59

60

61

62

Climatic and anthropogenic processes have significantly shaped the hydrological cycle and water availability over the last decades worldwide (Haddeland et al., 2014). Among them, climate change, land use changes, structural adaptation measures (e.g., levee systems and reservoirs), and deforestation have resulted in changes in streamflow at different spatial and temporal scales (Dev & Mishra, 2017). Land use changes profoundly impact regional water balances (Pielke et al., 2011), influencing interception, transpiration, evaporation, infiltration, and atmospheric blocking of precipitation, thus leading to changes in streamflow (Rogger et al., 2017; Tan et al., 2022). For instance, transforming vegetated areas into settlements may increase streamflow and reduce evapotranspiration (J. Du et al., 2012; Kundu et al., 2017; Wagner et al., 2013). Meanwhile, decreased areas under irrigated agriculture and decreased areas of forest cover have been associated with lower evapotranspiration and increased streamflow (Haddeland et al., 2006; Wagner et al., 2016). Augmenting irrigation results in a decline in streamflow through water withdrawals and an increase in water availability for evapotranspiration (Rost et al., 2008). Deforestation reduces evapotranspiration, leading to an increase in soil moisture and a decrease in soil storage capacity (Brown et al., 2005). Several areas of the contiguous United States (CONUS) have undergone substantial changes in land use due to many external factors such as land clearing, expansion of croplands, and urban growth (X. Li et al., 2023; Sohl et al., 2016). For example, the Corn Belt region has shifted from perennial grassland to annual row crops (Auch et al., 2018; Schilling et al., 2008). Forest extent has declined because of harvest, and shrubland and grassland have grown at the expense of this forest loss (Homer et al., 2020). Urban areas have shown a persistent increase, faster in southern states than in northern states (Homer et al., 2020). Future projections suggest rapid urban

expansion, some gain in forest cover, loss in pastures, and a possible increase in cropland, although these scenarios heavily depend on the underlying drivers of change (e.g., policy incentives, crop prices) (Lawler et al., 2014). Various studies have employed hydrological models to evaluate and project the impacts of land use on the hydrological cycle of various regions in the CONUS (e.g., Caldwell et al., 2012; Giri et al., 2019; Mishra et al., 2010; Parajuli et al., 2016). These studies have examined the impacts of diverse land uses on streamflow, encompassing shifts in cropping systems (Ahiablame et al., 2017; Frans et al., 2013; Schilling et al., 2008), irrigated agriculture (Ozdogan et al., 2010), and urbanization (C. Li et al., 2020). However, there is no consensus on the impact of land use changes on streamflow. For instance, Gupta et al. (2015) found a negligible influence of land use on increased streamflow in the midwestern USA. Meanwhile, Schilling (2016) and Schilling et al. (2008) have refuted this conclusion, asserting that the impacts of land use changes on streamflow in this region should not be neglected. These conflicting results highlight the research gaps in understanding the interactions between climate, hydrological processes, and land uses. The Budyko framework (Budyko, 1974) is a simple yet effective tool for evaluating how climate, surface characteristics, and land use interact and influence the water-energy balance. Under longterm steady-state conditions and negligible changes in water storage, the Budyko framework assumes that the water balance is primarily governed by the water supply (i.e., precipitation) and the water demand (i.e., potential evapotranspiration) (H. Li et al., 2020). However, deviations of measured data from the original Budyko curve have led to adopting parameterized versions, often using a single shape parameter (e.g., Choudhury, 1999; Fu, 1981; Pike, 1964; Turc, 1954; H. Yang et al., 2008). The shape parameter is named the catchment characteristic or landscape parameter,

63

64

65

66

67

68

69

70

71

72

73

74

75

76

77

78

79

80

81

82

83

and it captures the combined influence of climate factors beyond supply and demand, like geology, vegetation, topography, and human activities, including land use, on precipitation partitioning. Several studies have explored the relationship between the single shape parameter ω (Fu 1981) and diverse physical factors such as slope, elevation, vegetation, soil storage, etc. (e.g., Bai et al., 2020; D. Li et al., 2013; Liu & You, 2021; Xu et al., 2013). In the CONUS, Abatzoglou and Ficklin (2017) developed a generalized additive model of ω using topographic and climatic factors. Their model was built with 211 gages with minimal human influence, explaining 81.2% of the variability. However, when the model's performance was evaluated using 164 watersheds from the Model Parameter Estimation Project (MOPEX) with less stringent requirements in terms of human influence, the explained variability decreased to 65%. A previous study by Wang and Hejazi (2011) already pointed out that MOPEX watersheds are not free of human interferences and hypothesized possible relationships between streamflow change and human activities, such as irrigation or cropland area, but without a direct estimation of the effect or countereffects of these human activities on streamflow. A subsequent study by Z. Li and Quiring (2021b), relates the calibrated ω for 126 reference and 765 non-reference watersheds with physiographic and anthropogenic factors from the USGS database GAGES-II: Geospatial Attributes of Gages for Evaluating Streamflow (Falcone, 2011; Falcone et al., 2010). The authors concluded that forest coverage is important in representing spatial variability of ω in watersheds with limited human impact or reference watersheds. Meanwhile, urbanization is relevant in explaining spatial variability of ω in non-reference watersheds or watersheds with higher human imprints. While this study is a first attempt to quantify the contribution of different land uses and human activities in explaining the spatial variability of ω , the model's performance exhibited regional differences. These differences can be attributed to the limitations of a model for the entire CONUS to account

85

86

87

88

89

90

91

92

93

94

95

96

97

98

99

100

101

102

103

104

105

106

for regional variations in significant independent variables. A recent global-scale study by Liu and You (2021) showed that the factors explaining the spatial variability of ω vary by region, particularly with climate regions, highlighting the necessity of developing regional models of ω . However, this global scale study used non-human disturbed basins and natural catchment attributes.

Although these prior studies have provided valuable insights, to the best of our knowledge, none have examined how climatic and landscape factors (i.e., topography, vegetation, geology, and anthropogenic activities) interact and influence ω differently in human-impacted and non-human-impacted watersheds across various climatic regions within the CONUS. Additionally, previous studies have been limited in examining only a subset of these possible factors in the CONUS, mainly natural physiographic variables, despite the broad range of factors explored in the literature. Our study investigates the influence of anthropogenic activities and other catchment characteristics on the long-term water balance using the Budyko Framework for different climate zones in the CONUS, employing an extensive list of 49 factors. Specifically, this study focuses on how land use and its variability influence water-energy partitioning. We also identify which climates are more responsive to alterations in catchment characteristics, including land use changes. To accomplish this, we examine which variables, precipitation, potential evapotranspiration, or landscape factors account for the spatial distribution of mean annual streamflow in the CONUS.

The specific questions of this study are:

1. To what extent do climate variables and land uses explain the spatial heterogeneity of ω within climate regions?

2. What is the spatial variability in streamflow explained by climate and catchment characteristics in different climate regions?

To answer these questions, we classified watersheds in the CONUS by land use type and grouped them by climate region. Then, we calibrated ω from 1990 to 2020 using long-term hydroclimatic data. We calculated an extensive list of climatic, topographic, anthropogenic, vegetation, and geologic factors to select potential controls of ω . After, we developed stepwise multiple linear regression models to explore how a subset of these controls explains the spatial variability of ω within different climate regions. Finally, we computed the spatial variability on mean annual streamflow explained by precipitation, potential evapotranspiration, and ω also using linear regression models.

2 Materials and Methods

2.1 Hydro-climatic data and watershed classification

Streamflow gages from the GAGES-II database were selected for this study (Falcone, 2011; Falcone et al., 2010). The GAGES-II database provided geospatial data, environmental characteristics, and anthropogenic influences for 9067 basins in 9 ecoregions of the CONUS. Daily streamflow data from 1990 to 2020 were submitted to a completeness requirement to ensure data gaps do not bias results. Streamflow gages must have complete data (a daily value for every day of the year) for at least eight out of every ten years for each decade (e.g., 1990-1999) and a maximum of 10 days missing in the other two years (Dudley et al., 2020). A total of 3165 gages out of the 9067 met this criterion. We also discarded basins smaller than 300 km², reducing the streamflow gages for further study to 2193. We selected this threshold to strike a balance between

having sufficient watersheds in our sample and considering the spatial resolution of the climate 150 raster data used. 151 152 The 2193 basins were classified as either reference or non-reference watersheds according to their 153 anthropogenic alteration. Reference basins represent near-to-natural flow conditions, while nonreference basins are affected by human processes (e.g., urbanization). Non-reference basins were 154 155 further subdivided into urban, agricultural, or regulated, using the thresholds that Dudley et al. (2020) proposed (Table 1). A basin was classified as "Other" if it failed to meet any of the criteria. 156 Dudley et al. (2020) defined the high and low thresholds as the highest quartile and lowest half 157 158 values of the human activities (e.g., urban area, cultivated land) among the gages, respectively. 159 The 2019 National Land Cover Database (NLCD) (Dewitz & U.S. Geological Survey, 2021) is used to estimate the percentage of the basin used for cultivated crops and developed land. The 160 normalized dam storage is calculated as the normalized dam storage of the reservoirs in the 161 watershed multiplied by the drainage area and divided by the mean annual streamflow from 1990 162 to 2020. 163 Reference basins are minimally affected by direct human activities and belong to the USGS Hydro-164 Climatic Data Network 2009 (HCDN-2009) (Lins, 2012). There are 261 watersheds that belong to 165 the HCDN-2009, but only 158 of these watersheds met the low land-use thresholds in the 2019 166 NLCD. A total of 86 watersheds exceeded the limits of cultivated land and 40 the threshold of 167 168 urban land. Also, 23 watersheds have more than 60 days of normalized storage. This classification led to 158 reference gages, 68 urban gages, 172 agricultural gages, 209 regulated gages, and 1586 169 gages in the "Other" group (Table 1). Only reference, urban, and agricultural gages (a total of 398) 170 171 are used for subsequent analysis (Figure 1a), as regulated gages commonly violate the negligible change in storage assumption. 172

Both reference and non-reference basins were grouped in climate zones using the updated Köppen-Geiger climate classification at 1 km resolution by Beck et al. (2018). This updated map exhibits greater accuracy compared to previous versions due to their generation using topographically corrected climatic maps. Then, we grouped some of the climate zones using the criterion proposed by Liu and You (2021) (Table 2) to prevent groups with low numbers of watersheds while preserving the primary climate characteristics related to the temperature and precipitation of each Köppen-Geiger climate zone (Table S1). We selected the climate that covers the largest fraction of the watershed when the watershed area falls in more than one climate zone. This classification resulted in 5 climate groups (Table 2). A total of four watersheds that belonged to the Dwb climate (Cold, Dry winter, Warm summer) were excluded from the analysis due to insufficient sample size. The Mid-Atlantic and New England regions belong to Cold2, the South to Temperate2, the Great Plains and Midwest to Cold2 and Arid, the West Coast to Temperate1, and the Rocky Mountains to Cold1 (Figure 1b). Daily precipitation and reference evapotranspiration were extracted from gridMET (Abatzoglou, 2013) from 1990 to 2020 and averaged over each basin. The gridMET is a high-spatial-resolution (~4 km) gridded surface meteorological dataset, and it has been previously used in the context of the Budyko Framework in the CONUS (Abatzoglou & Ficklin, 2017; Guillén et al., 2021). There are several approaches to estimating the potential evapotranspiration, such as pan evaporation (Greve et al., 2015), the Penman-Monteith method based on a reference crop surface (Greve et al., 2020), or the Hargreaves-Samani method based on temperature (Istanbulluoglu et al., 2012). The reference evapotranspiration is the evapotranspiration for a short well-watered grass with a static albedo of 0.23 (Allen et al. 1998). This method follows the standardized ASCE approach and was also used by Abatzoglou and Ficklin (2017).

173

174

175

176

177

178

179

180

181

182

183

184

185

186

187

188

189

190

191

192

193

194

Table 1 Low and high thresholds for watershed classification into reference and non-reference (agricultural, regulated, or urban)

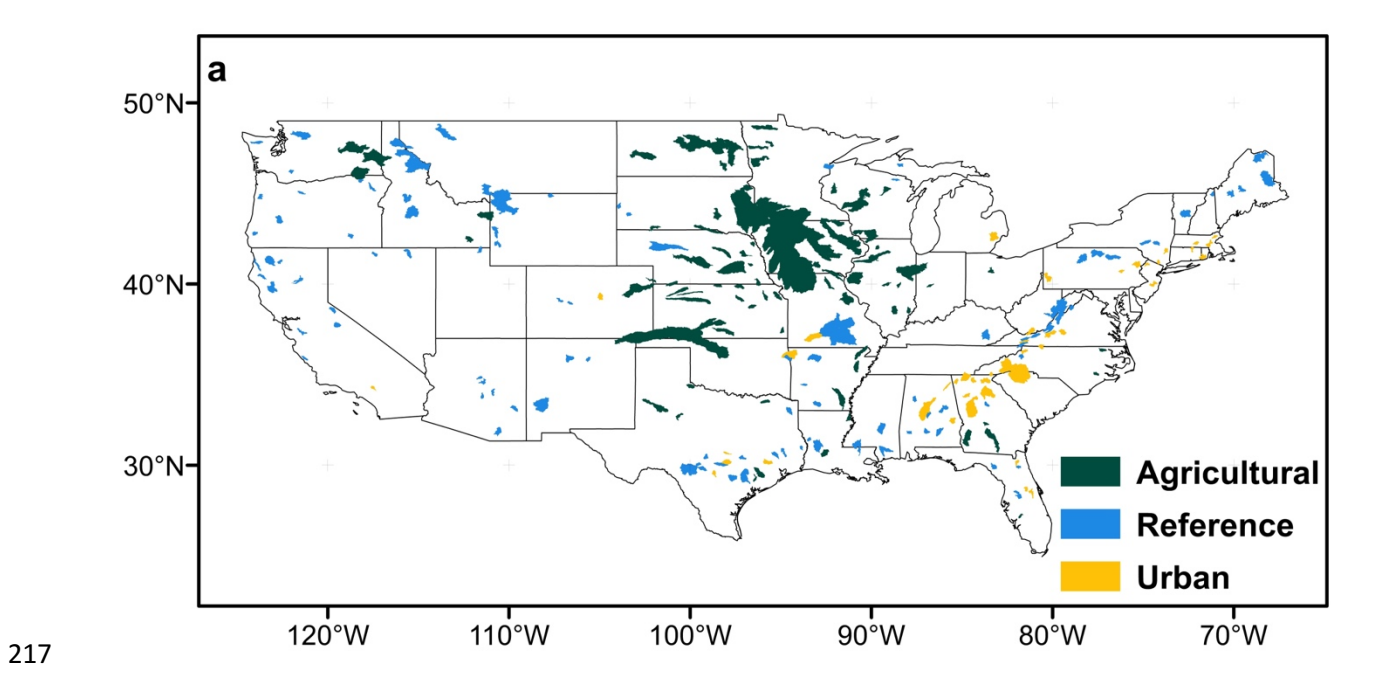
| Classification by land use and regulation HCDN-2009 | | High land-use threshold | Low land-use threshold | # watersheds |
|---|-----|---|---|-----------------|
| Reference | Yes | none | \leq 60 days normalized dam storage; \leq 6% developed land; \leq 2% cultivated crops | 158 |
| Agricultural No | | > 20% cultivated crops | 172 | |
| Regulated | No | > 180 days normalized dam storage | ≤ 2% cultivated crops; ≤ 6% developed land | 209 |
| Urban | No | > 10% developed land | \leq 2% cultivated crops; \leq 60 days normalized dam storage | 68 |

Table 2 Defining criteria of the Köppen-Geiger climate zones based on Beck et al. (2018) and Liu and You (2021)

| Classificatio n by climate | Code | Abbreviatio n | Precipitatio n type | Descriptio n | Definition | # watersheds |
|----------------------------|---------------------|---------------|-----------------------|--|--|--------------|
| | Dsc, Dsb | Cold1 | Dry summer | | $\begin{aligned} P_{sdry} &< 40 \& \\ P_{sdry} &< P_{wwet}/3 \end{aligned}$ | 23 |
| Cold | Dfa, Dfb, Dfc | Cold2 | Without dry season | Not Arid & $T_{hot} > 10 \& T_{cold} \le 0$ | $\begin{aligned} & \text{Not } (P_{\text{sdry}} < \\ & 40 \& \\ & P_{\text{sdry}} < P_{\text{wwet}} / 3) \\ & \text{or Not} \\ & (P_{\text{wdry}} < P_{\text{swet}} / 1 \\ & 0) \end{aligned}$ | 220 |
| | Csa, Csb | Temperate1 | Dry summer | Not Arid - & T _{hot} >10 | $\begin{aligned} P_{sdry} &< 40 \ \& \\ P_{sdry} &< P_{wwet}/3 \end{aligned}$ | 21 |
| Temperate | Cfa, Cfb | Temperate2 | Without dry season | $\begin{array}{c} & \text{α T_{hot}$-10} \\ & & 0 \\ & < T_{cold} < 18 \end{array}$ | Not $(P_{sdry} < 40 \& P_{sdry} < P_{wwet}/3)$ | 108 |

| | | | | | or Not | | |
|---------|------|--------|--------|--------------------------|------------------------|----|--|
| | | | | $(P_{wdry} < P_{swet}/1$ | | | |
| | | | | | 0) | | |
| الم شام | BSk, | Stanna | MAP<10 | MAP≥5 × | 22 | | |
| Arid | BSh | Arid | Steppe | $\times P_{threshold}$ | P _{threshold} | 22 | |

Note. MAP indicates the mean annual precipitation; T_{cold} and T_{hot} represent the average air temperature during the coldest and warmest months, respectively; P_{sdry} and P_{wdry} denote the precipitation in the driest months of summer and winter, respectively; P_{swet} and P_{wwet} represent the precipitation in the wettest months of summer and winter, respectively; and $P_{threshold}$ means the precipitation threshold. Units: MAP in mm y^{-1} ; Tcold and T_{hot} in ${}^{\circ}C$ and P_{swet} , P_{wdry} , and $P_{threshold}$ in mm.



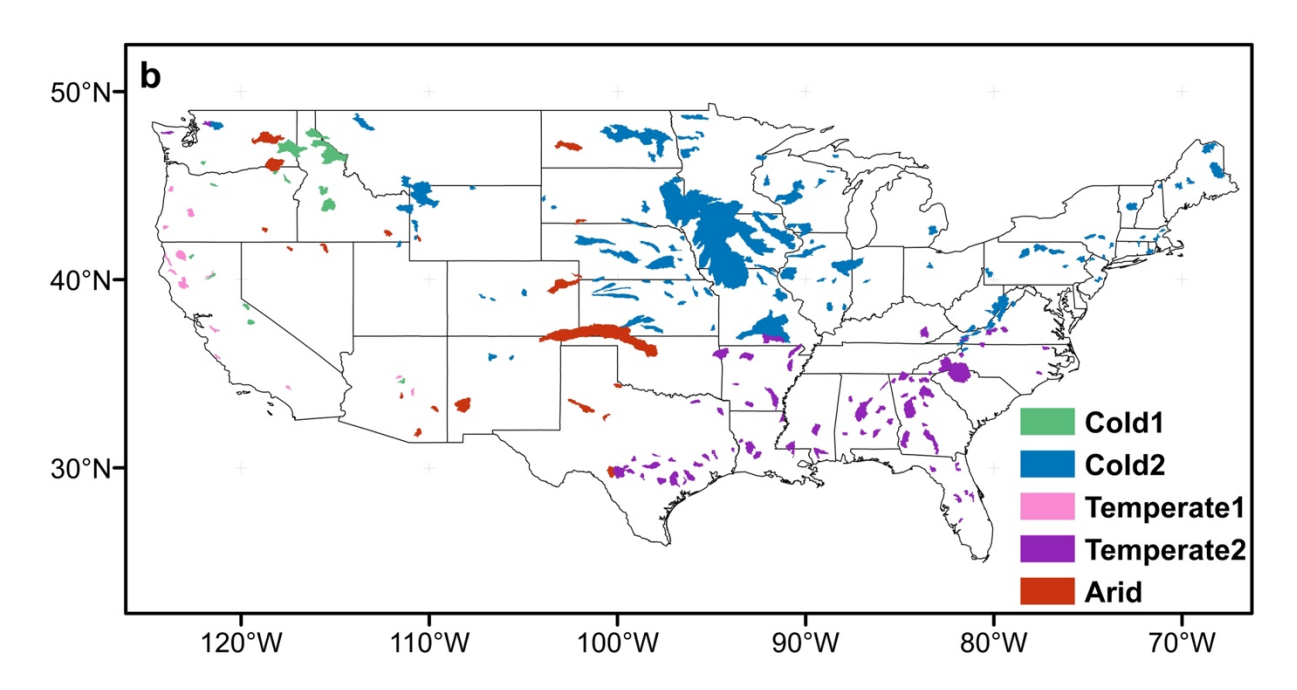


Figure 1 (a) Spatial distribution in the CONUS of the reference, agricultural, and urban watersheds and (b) grouped by climate

2.2. Water-energy balance

This study used the analytical form of the Budyko hypothesis proposed by Fu (1981), extensively implemented to study water-energy balances at different spatial and temporal scales (e.g., L. Cheng et al., 2011; C. Du et al., 2016; Greve et al., 2015; Koppa & Gebremichael, 2017; S. Li et al., 2022; Lv et al., 2019; Qiu et al., 2019; Sinha et al., 2019; L. Zhang et al., 2004; Zhao et al., 2020). The Fu equation estimates the watershed's long-term evapotranspiration (ET) as a function of the ratio between the available water (precipitation, P) and energy (potential evapotranspiration, PET), also called aridity index (ϕ), and the catchment characteristic parameter (ω). Fu's equation is expressed as follows:

$$\frac{ET}{P} = 1 + \frac{PET}{P} - \left[1 + \left(\frac{PET}{P}\right)^{\omega}\right]^{\frac{1}{\omega}} \tag{1}$$

where ω can be calibrated with historical P and streamflow (Q). When ω equals 2.6, Fu's curve corresponds to the traditional Budyko curve. High values of ω indicate watersheds where most of the P is used for ET. In contrast, low values of ω represent watersheds where a significant fraction of P becomes Q. For ω <2, watersheds have a higher sensitivity to land use factors relative to climate factors, whereas for ω >2, the climate factors tend to have greater importance (Zhou et al., 2015).

We calibrated ω for each watershed by minimizing the difference between the long-term mean ET (ET=P-Q) from 1990 to 2020 and the estimated ET by substituting the long-term mean P and PET into Fu's equation. We deemed a 31-year time frame sufficient to guarantee insignificant changes in storage. According to Z. Li and Quiring's (2021a) study, 84.4% of the 954 human-impacted watersheds they used from the GAGES-II database had a closed water balance for an 11-year time period. However, it is important to note that some watersheds, especially in arid catchments in the

western U.S., might have experienced storage changes due to groundwater withdrawals. Still, our sample size in this region is relatively small. The ω values were sampled from a uniform distribution from 1.25 to 9 with 0.01 increments, following the approach by Abatzoglou and Ficklin (2017). To ensure plausible water balances, we eliminated watersheds where Q>P or ET(P-Q)>PET (Peel et al., 2010). We also excluded watersheds with a calibrated ω equal to 1.25, as it represents the minimum value for bare soil (Donohue et al., 2012). Furthermore, we tested the hypothesis that ET/P and ω varies across different climate regions and land uses using the Kruskal-Wallis's test.

2.3. Selecting potential controls of ω

The literature provides an extensive list of controls that may govern ω , which can generally be classified into two groups: climate-based and landscape controls (Padrón et al., 2017; Shao et al., 2012; Vora & Singh, 2021). However, no primary control of ω has been defined to date because ω has no prior physical meaning (Greve et al., 2015). The selection of factors was based on a systematic review conducted by Padrón et al. (2017) that investigated ω 's controls at regional and global scales up until 2016. Additionally, we included the soil factors added to this review by Vora and Singh (2021) and other topographic and anthropogenic factors that Z. Li and Quiring (2021b) considered in their study conducted in the CONUS (Text S1). We computed 49 possible controls of ω classified into five categories, climatic (14), topographic (11), vegetation-related (5), anthropogenic (12), and geologic (7) (Table S2 and Table S3).

Given the large number of controls considered, we expect possible cross-correlations that could weaken the inference in determining the effect of each control. Therefore, we need first to select a

subset of potential controls of ω (Text S2). To do this, we evaluated the Spearman correlations

between ω and each control. We selected factors with the highest significant correlation with ω and highly correlated with the other factors in the same category (Table S4 and Figure S1). In this way, we eliminate internally correlated factors while assuming that the selected factors are sufficient to represent the excluded factors. Previous studies have used a similar approach (e.g., Vora & Singh, 2021). We selected ten variables to investigate their potential relationship with ω . These variables include relative cumulative moisture surplus (rCMS), fraction of precipitation falling as snow (SF), slope (Slope), forest cover (TreeCover), urban land (Settlements), cultivated land (Cultivated), irrigated agriculture (IrrAgri), percentage of urban land adjacent to a 100-meter width at each side of the main river (MAIN100DEV), number of dams in the watershed (NDams), and ratio of available water capacity in the top 1.5 meters of soil to precipitation (AWC0150:P). These ten variables became the independent variables against which omega was regressed in the stepwise multiple linear regression (SMLR) (Chu et al., 2019). All the retained variables in the SMLR are statistically significant at p-value<0.05 and have a Variance Inflation Factor<5 and tolerance>0.02. We normalized the dependent variable by applying a log transformation. Similarly, we applied either log or square root transformations for some of the independent variables that did not exhibit a linear relationship with ω . Subsequently, we standardized the independent variables by subtracting their mean and dividing them by their standard deviation. The standardization is done to assess variable importance. Finally, we validate the variance explained by the factors in the SMLR models by constructing 10,000 models through bootstrap sampling with replacement (Text S3).

265

266

267

268

269

270

271

272

273

274

275

276

277

278

279

280

281

282

283

284

2.4. Spatial variability of streamflow in different climate regions

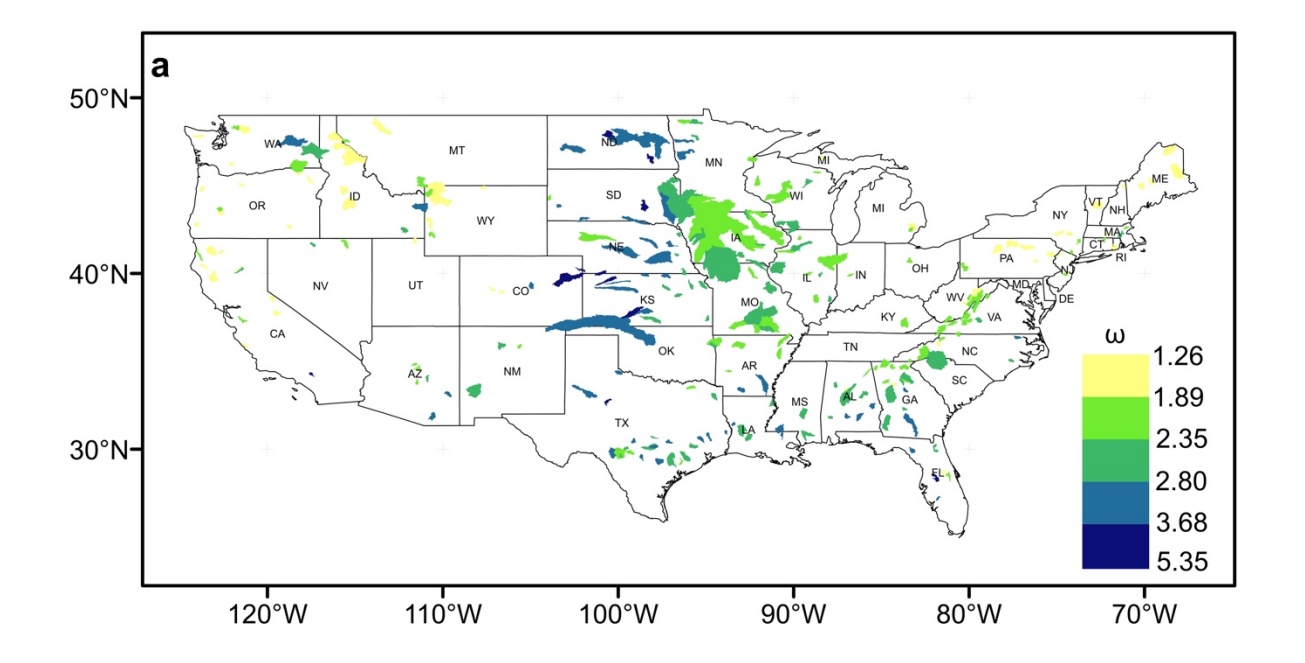
We assessed the spatial variability of mean annual Q explained by climate (i.e., P or PET) and catchment characteristics (i.e., ω) using SMLR. We created a SMLR for each climate region, using mean annual Q from 1990-2020 as the dependent variable and mean annual P, mean annual PET, and ω as predictors. To satisfy the requirement of constant variance in SMLR and to address an observed curvilinear relationship in the residuals versus fitted plot, we used quadratic terms for the variables P and PET instead of linear terms. All the retained variables in the SMLR are statistically significant at p-value<0.05 and have a Variance Inflation Factor<5 and tolerance>0.02. We also standardized the independent variables by subtracting their mean and dividing them by their standard deviation.

3 Results

3.1 Values of ω by climate region and land use

The total number of watersheds was reduced from 394 to 383, because for 4 watersheds ET>PET, and for 7 watersheds, ω equals 1.25. The climate zone has a significant influence on both ET/P (chi-squared or test statistic H of the Kruskal-Wallis's test = 70.29 and p-value<0.005) and ω (H = 71.52 and p-value<0.005). Also, the land use has a significant influence on both ET/P (H = 93.12 and p-value<0.005) and ω (H = 71.15 and p-value<0.005). Our values of ω across CONUS range between 1.26 and 5.35, with overall, ω >3 in the Great Plains and ω <2 in the Northeast and along the West Coast. The highest ω corresponds to arid basins with a mean value of 2.96, primarily located in the Great Plains and Midwest, and the lowest ω to basins in the dry summer cold climate (Cold1) with a mean value of 1.70, mainly found along the Rocky Mountains in Idaho (ID), Montana (MT) and Wyoming (WY) (Figure 2a). Forty-eight watersheds have values of ω higher

than 3 and are primarily located in the Great Plains (Figure 2a), belong to cold climate without dry season (Cold2) (Figure 3a), and are agricultural (Figure 3b). Despite being in a humid climate, these watersheds are in the water-limited region (ϕ >1) (Figure 2b); therefore, high values of ω are not unexpected. Only 25% of the humid climate watersheds (Cold2) are in the energy-limited region (ϕ <1) (Figure 3a) and are in the Mid-Atlantic and New England. In Temperate2, exposed to higher temperatures than Cold2, approximately 50% of watersheds are in the water-limited region, mainly in Florida (FL) and Texas (TX). The other 50% of watersheds in the energy-limited region are in the Appalachian Mountains and Mississippi (MS). We found similar variation when looking at the Temperate1 climate. Watersheds belonging to this group in the northwest (Oregon (OR) and Northern California (CA)) are in the energy-limited region. Meanwhile, watersheds in the southwest (Arizona (AZ) and Southern California (CA)) are in the water-limited region. Overall, temperate climates have slightly higher ω than cold climates (Figure 4a), and agricultural watersheds have higher ω , followed by urban and reference watersheds (Figure 4b).



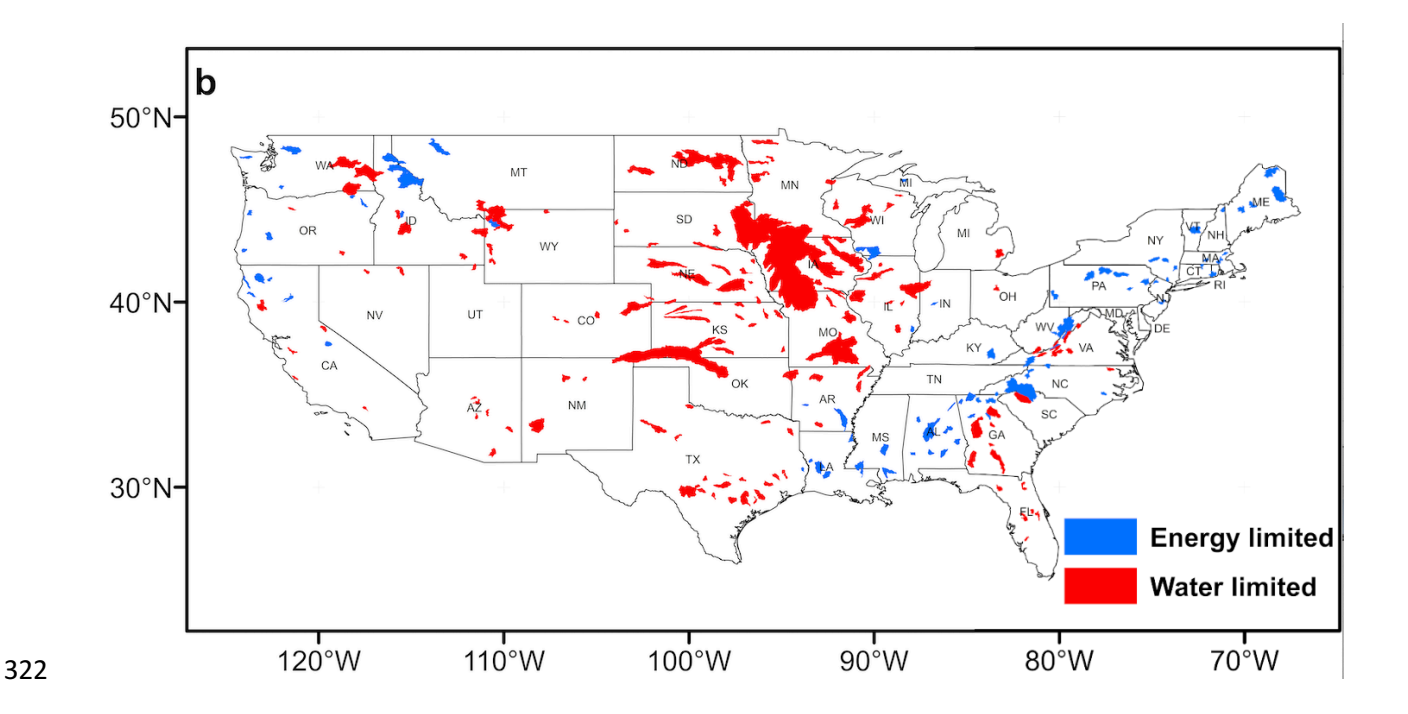


Figure 2 (a) Calibrated ω for the 1990–2020 period for the 383 watersheds; (b) Watersheds classified as energy limited (aridity index (ϕ) <1) or water limited $(\phi > 1)$

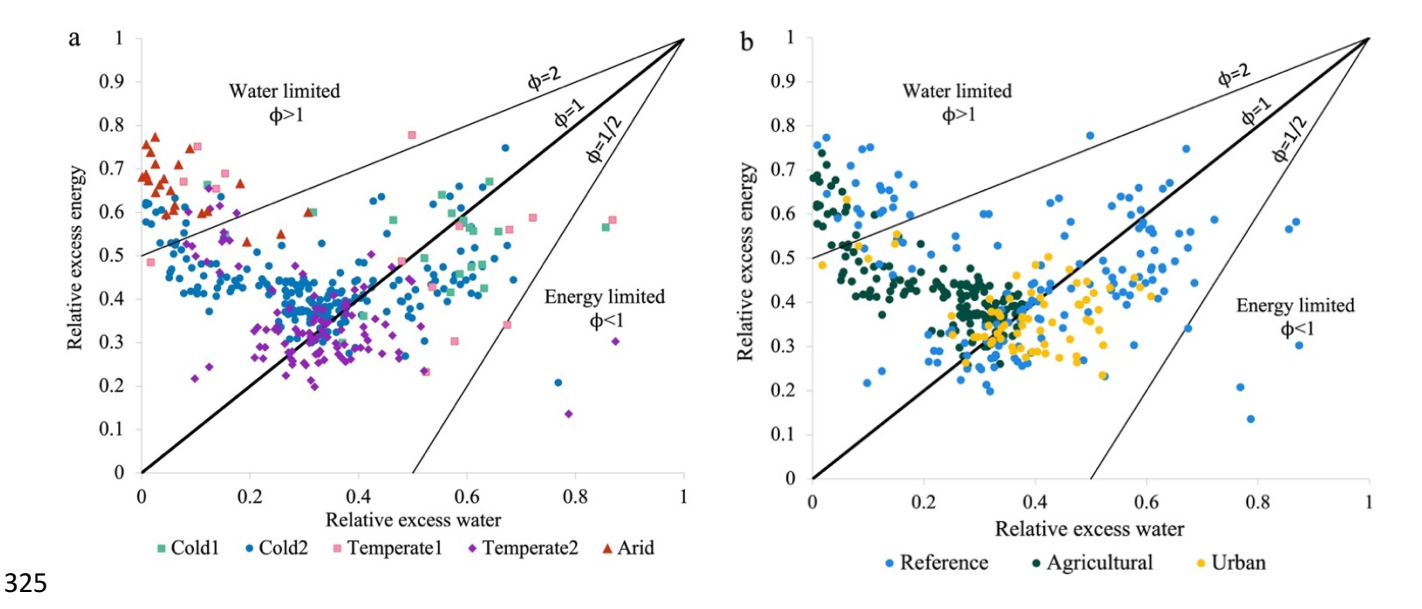


Figure 3 Diagram of relative excess energy (PET/ET) and relative excess water (1 - P/PET) with lines of constant aridity (ϕ) . The dot colors are the classification of watersheds based on (a) climate and (b) land use

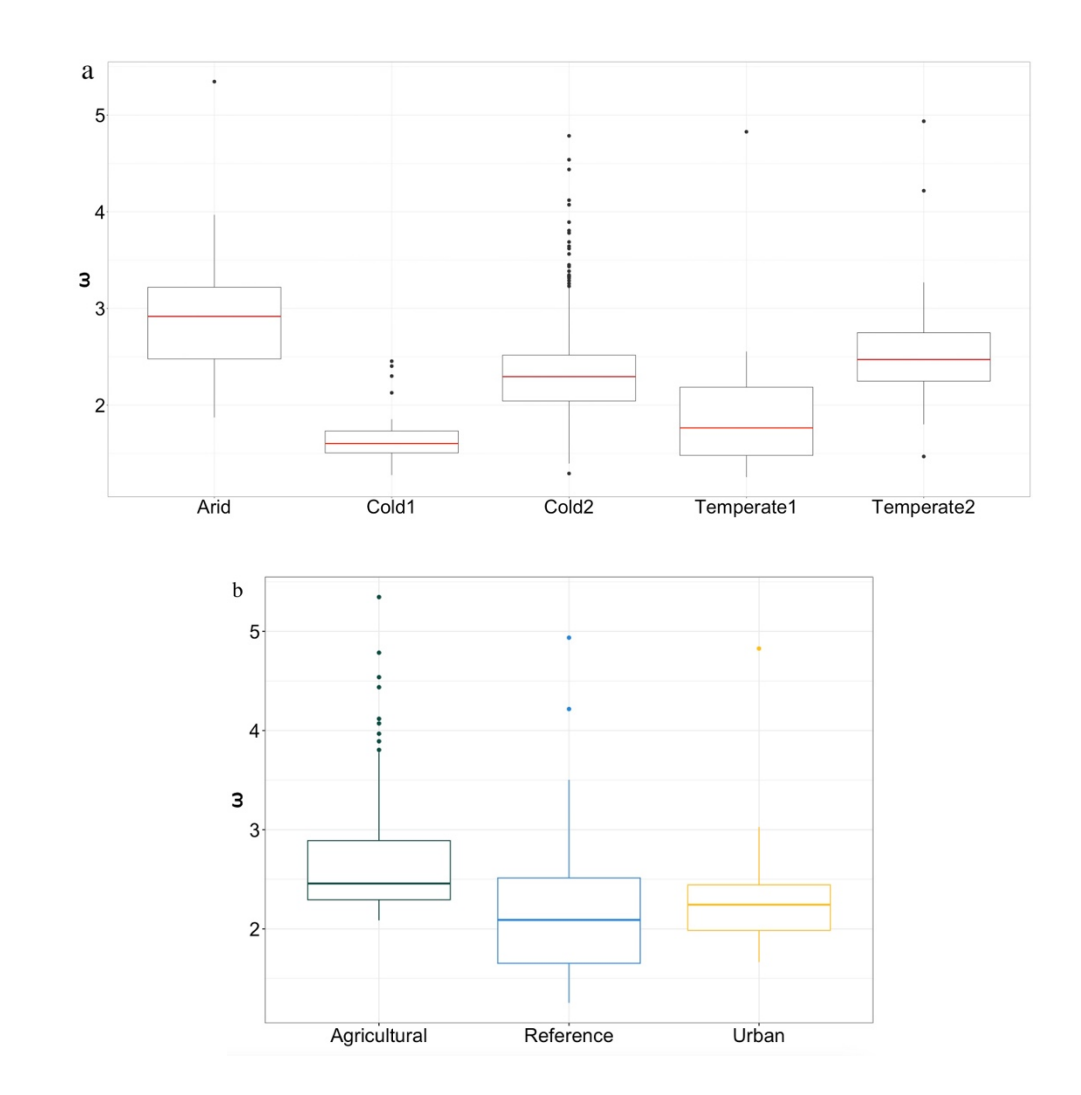


Figure 4 Boxplots of ω for (a) each climate region and (b) land use in the watershed. The middle line indicates the median, the box edges the 25th and 75th percentiles, and the dots are the outliers outside the whiskers at the 5th and 95th percentiles

3.2 Climate and landscape controls explaining spatial heterogeneity of ω by climate region

Different independent variables are identified as explanatory factors of the spatial variability in ω across the various climate zones (Table 3). In the Cold1 climate, the slope is the only significant factor with an adjusted R² of 0.43. Watersheds in the Cold1 climate, which exhibit the lowest ω ,

are predominantly located on the sides of the Rocky Mountains in Idaho, and have the steepest slopes among all watersheds, ranging between 18° and 28°. Conversely, watersheds in the same climate group, located along the west coast in California and Oregon, display higher ω values and are marked by less steep slopes. Within the Cold2 climate, we have identified four factors that collectively account for 76% of the spatial variability in ω . These factors include two climatic controls, one human-related control, and one soil-related control. Among these, the most influential is the relative cumulative moisture surplus (rCMS), which represents the synchronization between P and PET. This factor explains 65% of the variability alone. Geographically, P and PET display lower synchronization (higher rCMS) in the Northwest and Northeast leading to increased O, and higher synchronization (lower rCMS) in the Midwest (Figure 5). The second most significant factor, though considerably less impactful than rCMS, is irrigated agriculture (IrrAgri), explaining 7% of the variability. Noteworthy agricultural watersheds with substantial irrigated land, such as Nebraska and Kansas (Dieter et al., 2018), exhibit a mean ω above 3. Conversely, watersheds in Iowa, North Dakota, and South Dakota, characterized by extensive cultivated land but minimal irrigated land, display an average ω below 3. Additionally, the available water for plants (AWC0150:P) and the snow fraction (SF) explained a residual variance. AWC0150:P is higher in the Midwest compared to the Northwest and Northeast regions (Figure 5), favoring higher ET due to increased water retention in the soil. In the northern part of the Midwest (North Dakota, South Dakota, and Minnesota) and Northwest, SF is higher favoring Q (Figure 5). In the Temperate 1 climate, rCMS explains around 40% of the ω 's spatial variability. The values of rCMS show a decreasing trend as we move from Oregon, where it reaches a maximum, along

the west coast, reaching its lowest value in Arizona. Watersheds in Oregon exhibit a higher phase

339

340

341

342

343

344

345

346

347

348

349

350

351

352

353

354

355

356

357

358

359

360

shift P and PET, whereas in California and Arizona, P and PET are more seasonally synchronized, or PET sometimes exceeds P. The urban land in the riparian zone (MAIN100DEV), explains around 20% of the variability. This finding can be attributed to the distinctive characteristics of the urban watershed within this group, which stands out due to its high percentage of MAIN100DEV land and the highest value of ω . Within the Temperate 2 climate, slope is the most important factor, explaining 29% of the ω 's spatial variability. Watersheds along the Appalachian Mountains exhibit the highest slopes within the group, ranging from 5° to 20° (Figure 6), with an average ω below 2.3. The level of urbanization (Settlements) served as a second factor, explaining 11% of the ω 's spatial heterogeneity. Highly urbanized watersheds (>40% of the watershed's area) are concentrated in South Carolina, Georgia, and Alabama and have an average ω of 2.1. Urbanization leads to increased streamflow, potentially due to reduced infiltration and soil moisture storage (O'Driscoll et al., 2010). SF accounts for a negligible variance, contributing only 3%. The watersheds in the Appalachian Mountains and Ouachita-Ozark Mountains in Arkansas have higher average SF values compared to those in the Coastal Plains (Figure 6). In arid regions, rCMS explains 63% of the total ω 's spatial variability, while the slope accounts for 13% of the total variability, which amounts to 76%. Arid watersheds in the southwest regions of Arizona, New Mexico, and Nevada, as well as the Northwest in Oregon, exhibit higher slopes and rCMS values, resulting in lower ω values compared to arid watersheds in the Great Plains. The findings of the SMLR models constructed using bootstrapping sampling (Text S3) validate the variance explained by the controls (Table 3). We observed nearly identical average variances explained by each control when utilizing 10,000 SMLR models constructed via bootstrapping,

362

363

364

365

366

367

368

369

370

371

372

373

374

375

376

377

378

379

380

381

382

compared to using the original dataset. Nonetheless, discrepancies increase as the variance explained by the control decreases.

Table 3 SMLR results for each climate region using ten controls of ω . The Cumulative Adj. R² represents the incremental Adj. R² added to the model with the inclusion of each variable and AIC is the Akaike Information Criterion of the model

| Climate | Variable | Coeff | Std. Error | t- value | Pr (> t) | p-value model | Cum. Adj. R ² | Adj. R ² | AIC |
|-------------|-------------|-------|---------------|---------------|---------------|------------------|--------------------------------|------------------------|---------|
| Cold1 | Slope | -0.12 | 0.03 | -3.99 | 7.82e-04 | 7.82e-04 | 0.43 | 0.43 | -81.53 |
| | rCMS | -0.12 | 0.01 | -9.96 | < 2.2e- 16 | | 0.65 | 0.76 | -314 |
| Cold2 | IrrAgri | 0.03 | 0.01 | 3.09 | 0.002 | < 2.2e-16 | 0.72 | | |
| | AWC0150:P | 0.08 | 0.02 | 5.40 | 1.77e-07 | | 0.73 | | |
| | SF | -0.05 | 0.01 | -4.85 | 2.37e-06 | | 0.76 | | |
| Tommonoto 1 | rCMS | -0.23 | 0.05 | -4.30 | 1.03e-03 | 6.63e-05 | 0.40 | 0.61 | 0.21 |
| Temperate1 | MAIN100DEV | 0.25 | 0.04 | 5.91 7.11e-05 | 0.036-03 | 0.61 | 0.61 | 0.21 | |
| | Slope | -0.07 | 0.02 | -4.29 | 4.05e-05 | | 0.29 | | |
| Temperate2 | Settlements | -0.06 | 0.01 | -4.94 | 3.09e-06 | 2.33e-13 | 0.40 | 0.43 | -132.35 |
| | SF | -0.04 | 0.02 | -2.32 | 0.022 | - | 0.43 | - | |
| Arid | rCMS | -0.14 | 0.03 | -4.66 | 1.69e-04 | - 1.05e-06 | 0.63 | 0.76 | 15.06 |
| Afiq | Slope | -0.11 | 0.03 | -3.99 | 7.80e-04 | 1.036-06 | 0.76 | | 13.06 |

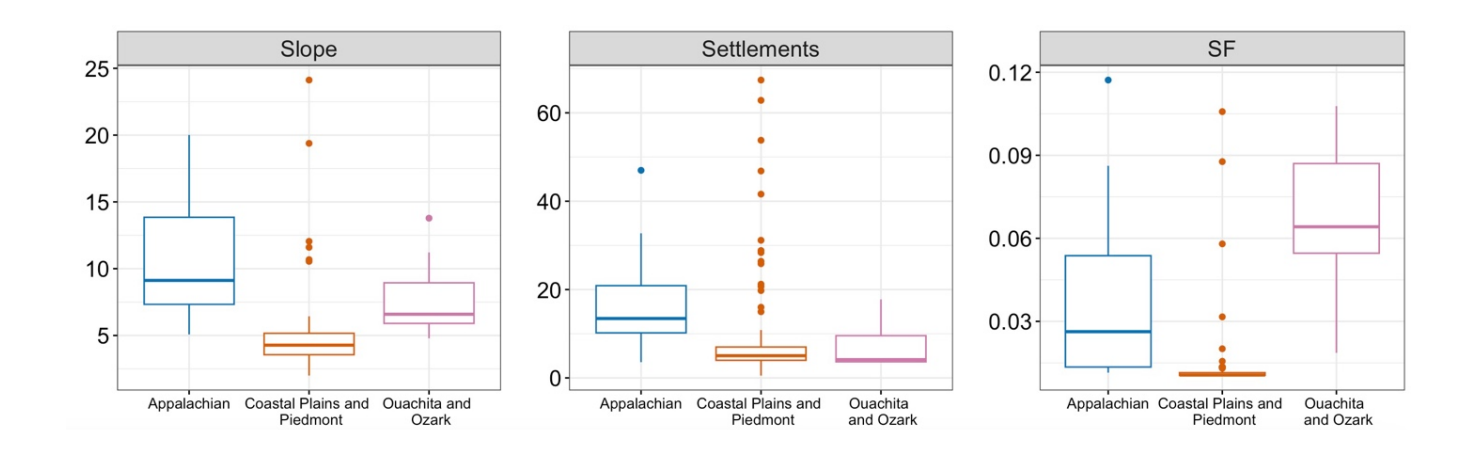


Figure 5 Boxplot of climatic variables explaining spatial heterogeneity of ω for Cold2 climate across the three geographical regions

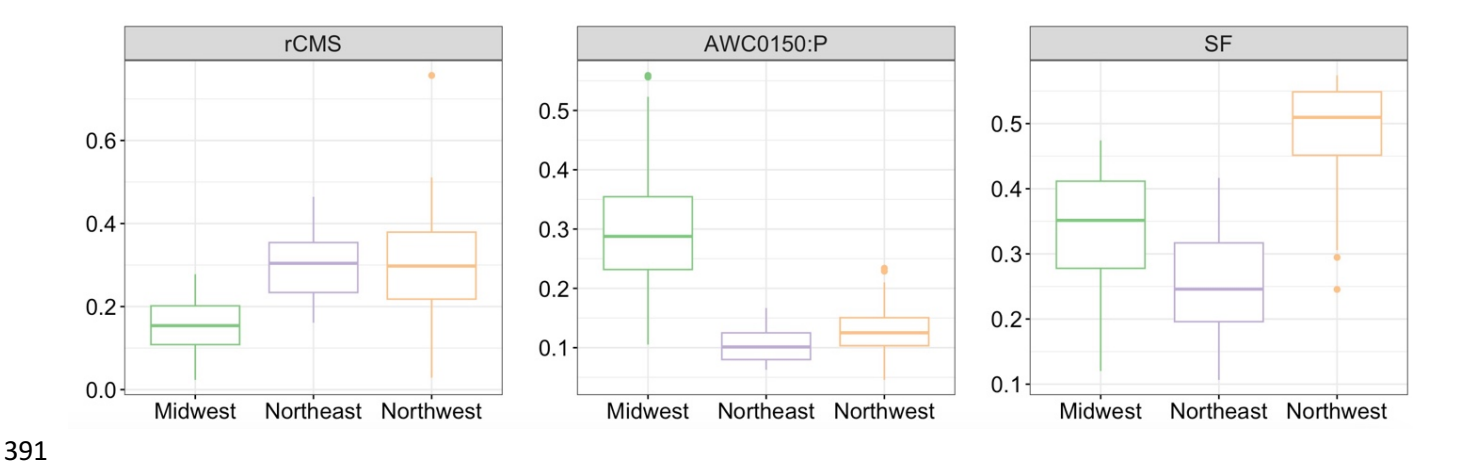


Figure 6 Boxplot of variables explaining spatial heterogeneity of ω for Temperate2 climate across different geographical regions

3.3 Spatial variability of streamflow explained by climate and catchment characteristics across different climate regions

The spatial variability of streamflow, attributed to climate and catchment characteristics, differs across various climate regions (Table 4). Precipitation accounts for more than 80% of the spatial variance in mean annual Q in all the climates, except in arid climates, where it only explains about 16%. The catchment characteristics (ω) exhibit the most substantial influence on the spatial variance of mean annual Q in arid climates, explaining up to 48% of the variability, which is considerably higher than the other climates. In the Cold2 climate, catchment characteristics explain

10% of the spatial variance on mean annual Q, while in the remaining climates, the percentage of spatial variance explained by ω is below 10%.

Table 4 SMLR results for each climate region using Q as dependent variable and P, PET, and ω as independent variables. Var is the variable P, PET or ω . The Cumulative Adj. R² represents the incremental Adj. R² added to the model with the inclusion of each variable and AIC is the Akaike Information Criterion of the model.

| Climate | Var. | Coefficient | Std. Error | t-value | Pr (> t) | p-value model | Cumula tive Adj. R ² | Adj. R ² model | AIC |
|------------|------|-------------|---------------|---------|-----------|------------------|---------------------------------------|---------------------------------|--------|
| | P | 0.87 | 0.03 | 26.31 | 3.2e-15 | | 0.91 | | |
| Cold1 | ω | -0.26 | 0.02 | -10.62 | 6.4e-09 | < 2e-16 | 0.98 | 0.99 | -31.46 |
| | PET | -0.06 | 0.02 | -2.62 | 0.018 | | 0.99 | | |
| | P | 0.69 | 0.03 | 27.47 | < 2e-16 | _ | 0.81 | | · |
| Cold2 | ω | -0.28 | 0.03 | -10.73 | < 2e-16 | < 2e-16 | 0.91 | 0.93 | 59.93 |
| | PET | -0.11 | 0.02 | -5.36 | 2.1e-07 | | 0.93 | | |
| | P | 0.77 | 0.06 | 11.98 | 1.2e-07 | _ | 0.93 | 0.98 | -8.53 |
| Temperate1 | ω | -0.14 | 0.05 | -3.13 | 0.009 | 8.5e-10 | 0.97 | | |
| | PET | -0.18 | 0.07 | -2.67 | 0.02 | | 0.98 | | |
| | P | 0.87 | 0.03 | 26.72 | < 2e-16 | _ | 0.94 | | |
| Temperate2 | ω | -0.13 | 0.01 | -21.58 | < 2e-16 | < 2e-16 | 0.98 | 0.99 | -181.9 |
| | PET | -0.11 | 0.01 | -8.64 | 8.1e-14 | | 0.99 | | |
| | ω | -0.29 | 0.08 | -3.42 | 0.003 | _ | 0.48 | | |
| Arid | P | 0.47 | 0.11 | 4.26 | 0.0004 | 2.0e-05 | 0.64 | 0.79 | 36.77 |
| | PET | -0.36 | 0.10 | -3.55 | 0.002 | - | 0.79 | | |

4 Discussion

4.1. To what extent do climate variables and land uses explain the spatial heterogeneity of ω within climate regions?

Our analysis reveals that climatic variables, specifically the phase shift between P and PET, are more relevant in humid climates in the Northeast and Midwest (Cold2 climate) and arid climates

in the Southwest and Great Plains relative to other areas. In contrast, in other climates, topographic variables, such as slope, appear to be more important, notably in the Southeast (Temperate2 climate) and Northwest (Cold1 climate) (Table 3). This finding aligns with our expectations, as we observed variations in the Spearman correlations between ω and these factors across different climates (Table S4). Our Spearman correlations between ω and the climatic factors for the Cold2 climate (i.e., 0.72 for AWC0150:P and -0.77 rCMS, Table S4), which represents the largest group, align in magnitude with those reported by Abatzoglou and Ficklin (2017) for the entire CONUS. However, these correlations significantly diminish in other climates. Hence, using the same factors to predict ω in the entire CONUS overlooks distinctions in the roles of climatic and landscape factors to explain regional differences in water balances. Abatzoglou and Ficklin (2017)'s model for the entire CONUS attributed a nominal influence of slope on ω . However, our findings demonstrate its relevance, particularly in Cold1 and Temperate2 climates, where the Rocky Mountains and Appalachian Mountains are located. Meanwhile, Guillén et al. (2021) determined that elevation as the primary landscape factor in their localized study of watersheds in the Appalachian Mountains due to the direct positive relationship between altitude and precipitation. These differences demonstrate the scale-dependent nature of the factors governing precipitation partitioning. Consequently, factors like elevation or snow might have minimal influence on broader regional climate patterns but still affect precipitation partitioning at smaller, localized scales. A novelty of this study is our emphasis on anthropogenic activities, which extends previous research using the Budyko framework focused on studying non-human modified basins. In the CONUS, Wang and Hejazi (2011) hypothesized about the potential influence of human activities (e.g., dam storage, population density, cropland area) on streamflow changes. Meanwhile, Z. Li

417

418

419

420

421

422

423

424

425

426

427

428

429

430

431

432

433

434

435

436

437

438

and Quiring (2021b) observed that factors explaining spatial differences in ω differ between human-impacted and non-human-impacted watersheds. Z. Li and Quiring (2021b) found that dam storage and urbanization better represent the spatial heterogeneity of ω in human-impacted watersheds. In this study, the number of dams does not appear to be a significant factor in any of the SMLRs, which may be attributed to the exclusion of regulated watersheds from the analysis. We found that in the climates with the largest sample of watersheds (Cold2 and Temperate2 climates), different anthropogenic activities account for spatial differences in the long-term water balances, as agricultural watersheds concentrate in the Cold2 climate and urban watersheds in the Temperate2 climate. This highlights the importance of climate regions in shaping the effects of land use change on streamflow generation and emphasizes the need to build regional models of ω . Over the period from 1990 to 2020, irrigated agriculture in the Midwest and Central Plains has intensified ET, while urban areas in the Southeast have increased Q. Water balances in humid watersheds of the Northeast and Midwest and arid watersheds of the Southwest and Great Plains are driven by the synchronization between P and PET (Table 3). Consequently, any shift in the seasonal dynamics of P and PET can greatly impact droughts and freshwater availability in these regions. Agricultural watersheds in the Midwest have benefited from a strong synchronization between P and PET complemented by their capacity to retain soil moisture (Figure 5). However, the region may encounter challenges in the future due to rising warm-season temperatures and the increasing occurrence of more variable and extreme precipitation events (Angel et al., 2018). These shifts in P and PET patterns could lead to excess soil moisture in the spring caused by increased precipitation, followed by insufficient levels during the summer growing season due to elevated temperatures (Wehner et al., 2017). Increased humidity in the spring, resulting in increased rainfall, is also associated with a higher frequency of

440

441

442

443

444

445

446

447

448

449

450

451

452

453

454

455

456

457

458

459

460

461

flooding events (Angel et al., 2018), posing risks to both the population and agriculture fields (Wing et al., 2018). Concurrently, rising temperatures will lead to an increased vapor pressure deficit, compelling farmers to extend their irrigation areas, which currently rely on rain, to maintain crop productivity since precipitation is not expected to increase at the same rate (DeLucia et al., 2019; Overpeck & Udall, 2020). Szilagyi (2018) found that, in the most extensively irrigated fields in Nebraska, ET rates have increased by 7mm decade⁻¹ from 1979 to 2015 along with a reduction of P. This phenomenon occurred because irrigation resulted in a more stable air stratification over the cooler irrigated crop surfaces, ultimately causing the excess moisture to be dropped somewhere downwind. This study shows that irrigated agriculture explains 7% of the spatial variability in ω in the Midwest (Table 3), with a correlation coefficient of 0.6 (p-value<0.05) (Table S4). Therefore, the anticipated increase in irrigation will further intensify ET under high-temperature days when evaporative demand is the greatest, consequently exacerbating the long-term aridification of these watersheds. Spatial differences in water balances across the Southeast can be attributed to the watershed's slope and level of urbanization. The Southeast is experiencing significant urbanization, with some of the fastest-growing cities in the USA, particularly in swiftly developing urban centers in Florida, North Carolina, and South Carolina. This region has also experienced an increase in the frequency and intensity of precipitation events, and this trend is projected to persist in the future (Easterling et al., 2017). Urbanization in the Southeast has been linked to processes that amplify intense rainfall events, such as urban heat island dynamics or elevated aerosol production, and it has also led to higher runoff ratios and peak flows (Ashley et al., 2012; O'Driscoll et al., 2010). For instance, Diem et al. (2018) showed a 26% increase in annual streamflow and a rise in runoff ratio from 0.35 to 0.45 due to urbanization in some watersheds in the Atlanta Metropolitan area from 1986

463

464

465

466

467

468

469

470

471

472

473

474

475

476

477

478

479

480

481

482

483

484

to 2015. C. Li et al. (2020) reported that the southeastern US exhibits a more pronounced hydrological response to urbanization compared to other regions in the CONUS, resulting in a higher water yield due to the expansion of impervious areas and loss in vegetated areas. In this study, we found that in the Southeast, the urban area within the watershed accounts for 11% of the spatial variability in ω between 1990 and 2020 (Table 3), with a correlation coefficient of -0.22 (p-value<0.05) (Table S4). In the other climate groups, the sample size constrains the range of variability of the controls, thereby limiting the interpretation of the SMLRs. We selected a subset of factors to regress against ω ; however, due to the unknown nature of ω and the broad range of factors that may influence it, we acknowledge that this selection can be somewhat subjective. However, it is important to note that the parameter ω is highly correlated with the selected controls, which are also highly crosscorrelated with the other controls in the same category (Figure S1), meaning that they represent similar hydrological processes. Also, the significant relationship between the selected controls and ω indicates that modification of these controls can affect precipitation partitioning. In this analysis, we used ω as a proxy of ET/P to regress against the controls; by doing so, we introduced some uncertainties, especially when a catchment reaches the water and energy limits (Reaver et al., 2022). Nevertheless, employing ω as the dependent variable instead of ET/P enables the identification of controls beyond those exerted by ϕ . While we relied on past studies to assess the closed water balances (i.e., Z. Li & Quiring, 2021a), we recognize a limitation that certain human-

486

487

488

489

490

491

492

493

494

495

496

497

498

499

500

501

502

503

504

505

506

507

The groundwater depletion is more notable in semiarid to arid watersheds in the western US

affected basins might have undergone alterations in water storage due to groundwater withdrawals.

(Konikow, 2013), but our sample size in this region is relatively small.

4.2. What is the spatial variability in streamflow explained by climate and catchment characteristics in different climate regions?

508

509

510

511

512

513

514

515

516

517

518

519

520

521

522

523

524

525

526

527

528

529

530

Our results indicate that arid climates are especially sensitive to changes in the catchment characteristics represented by ω . Specifically, ω explains around half of the spatial variability in the mean annual Q of arid catchments, meanwhile, mean annual P explains less than one-fourth (Table 4). In arid regions, alterations to forest cover or other land-use/land-cover types can result in more significant streamflow changes. Also, past research has found that streamflow is more responsive to land use and vegetation changes in arid regions (Wang & Hejazi, 2011; S. Zhang et al., 2016; Zhou et al., 2015; Bhaskar et al., 2020). For example, vegetation shows higher sensitivity to precipitation in dry regions, leading to an increase in vegetation cover, soil moisture, and changes in water availability (Y. Zhang et al., 2022). It is also important to note that ω encompasses other factors beyond anthropogenic activities, such as changes in topography, soil characteristics, precipitation patterns, and temperature. These factors also influence ω but typically involve longer-term processes (i.e., erosion, climate change) and are considered relatively more stable over time than rapidly changing human-induced activities (i.e., land use changes). To better assess the sensitivity of arid regions to land use changes, future research should investigate a larger number of watersheds affected by diverse land use/land cover alterations (e.g., urban expansion, deforestation). The sample we studied within this region is relatively small, with half of the watersheds categorized as reference or free from human intervention. Cold and Temperate climates, on the other hand, are primarily driven by the mean annual P, although cold climates show slightly higher sensitivity to changes in ω than temperate climates. This finding helps reconcile contradictions in the literature by demonstrating that some climates are more sensitive to changes in catchment characteristics, including land use and land cover changes, than others.

Climate has a significant influence on ω and ET/P ratio in the CONUS, as observed in other intraregional (Guillén et al., 2021) and global studies (Liu & You, 2021; Padrón et al., 2017). Arid regions exhibit the highest ω values, followed by temperate and cold regions. These findings highlight how climate groups can account for a portion of the spatial variability in ω across the CONUS, although there are broad ranges of ω within groups (Figure 4a). Land use also exerts a significant influence on ω and ET/P ratio in the CONUS. Agricultural watersheds display the highest ω values, while reference watersheds display higher dispersion (Figure 4b). Most of the watersheds (72%) in humid climates (Cold1 and Cold2) and half in temperate climates (Temperate 1 and Temperate 2) are water-limited and not energy-limited, contradicting commonly held assumptions (Figure 3a). We found that humid watersheds falling within the water-limited spectrum are mainly agricultural and concentrated in the Midwest, whereas water-limited watersheds in the temperate climate are primarily urban and spread across the South. We showed that there are complex interactions between climate factors and agricultural-urban factors that make the effect of land use different across climates. By building regional models of ω , we gained insight into how land use contributes to disparities in water balances within distinct climate regions. Our findings provide valuable insights into the critical factors to consider in the management of regional water resources and inform about the hydrological sensitivities to future climate and land use changes.

CRediT author statement

Conceptualization,

Hornberger:

531

532

533

534

535

536

537

538

539

540

541

542

543

544

545

546

547

548

549

550

551

552

Data Curation, Visualization, Writing - Original Draft, Writing - Review & Editing. George M.

Writing

Review

Sara Alonso Vicario: Conceptualization, Methodology, Software, Formal analysis, Investigation,

553 Supervision. **Maurizio Mazzoleni**: Conceptualization, Methodology, Writing - Review &

Methodology,

Editing,

Editing, Supervision. Margaret Garcia: Conceptualization, Methodology, Writing - Review &
 Editing, Project administration, Resources, Funding acquisition, Supervision.

Competing interests

The authors declare that they have no conflict of interest.

Acknowledgments

This work was supported by the National Science Foundation Grant Transition Dynamics in Integrated Urban Water Systems (Grant Number 1923880).

Data Availability Statement

All data used in the study are freely available for academic research in the public domain. The GAGES-II data set is available from https://water.usgs.gov/GIS/metadata/usgswrd/XML/gagesII_Sept2011.xml. The streamflow data is available from https://waterdata.usgs.gov/nwis. The gridMET data set is available from https://www.climatologylab.org/gridmet.html. References to other data can be found in the sources cited in Table S2 and Table S3 of the Supplementary material. A list of the gauging stations and the controls used in the SMLR models can be found in Table S5 of the Supplementary material. The values for the remaining controls are available upon request to the corresponding author.

References

- Abatzoglou, J. T. (2013). Development of gridded surface meteorological data for ecological
- applications and modelling. *International Journal of Climatology*, 33(1), 121–131.
- 574 https://doi.org/10.1002/joc.3413
- Abatzoglou, J. T., & Ficklin, D. L. (2017). Climatic and physiographic controls of spatial
- variability in surface water balance over the contiguous United States using the Budyko
- relationship. *Water Resources Research*, *53*(9), 7630–7643.
- 578 https://doi.org/10.1002/2017WR020843
- Ahiablame, L., Sinha, T., Paul, M., Ji, J. H., & Rajib, A. (2017). Streamflow response to
- potential land use and climate changes in the James River watershed, Upper Midwest
- United States. *Journal of Hydrology: Regional Studies*, *14*, 150–166.
- 582 https://doi.org/10.1016/j.ejrh.2017.11.004
- Allen, R., Pereira, L., Raes, D., & Smith, M. (1998). Crop evapotranspiration: Guidelines for
- Computing Crop Water Requirements (56). https://www.fao.org/3/x0490e/x0490e00.htm
- Angel, J. R., Swanson, C., Boustead, B. M., Conlon, K., Hall, K. R., Jorns, J. L., Kunkel, K. E.,
- Lemos, M. C., Lofgren, B. M., Ontl, T., Posey, J., Stone, K., Takle, E., & Todey, D. (2018).
- Chapter 21: Midwest. Impacts, Risks, and Adaptation in the United States: The Fourth
- National Climate Assessment, Volume II. https://doi.org/10.7930/NCA4.2018.CH21
- Ashley, W. S., Bentley, M. L., & Stallins, J. A. (2012). Urban-induced thunderstorm
- modification in the Southeast United States. *Climatic Change*, 113(2), 481–498.
- 591 https://doi.org/10.1007/s10584-011-0324-1

- 592 Auch, R. F., Xian, G., Laingen, C. R., Sayler, K. L., & Reker, R. R. (2018). Human drivers,
- biophysical changes, and climatic variation affecting contemporary cropping proportions in
- the northern prairie of the U.S. *Journal of Land Use Science*, 13(1–2), 32–58.
- 595 https://doi.org/10.1080/1747423X.2017.1413433
- Bai, P., Liu, X., Zhang, D., & Liu, C. (2020). Estimation of the Budyko model parameter for
- small basins in China. *Hydrological Processes*, *34*(1), 125–138.
- 598 https://doi.org/10.1002/hyp.13577
- Beck, H. E., Zimmermann, N. E., McVicar, T. R., Vergopolan, N., Berg, A., & Wood, E. F.
- 600 (2018). Present and future köppen-geiger climate classification maps at 1-km resolution.
- 601 Scientific Data, 5, 180214. https://doi.org/10.1038/sdata.2018.214
- Brown, A. E., Zhang, L., McMahon, T. A., Western, A. W., & Vertessy, R. A. (2005). A review
- of paired catchment studies for determining changes in water yield resulting from
- alterations in vegetation. *Journal of Hydrology*, 310(1–4), 28–61.
- 605 https://doi.org/10.1016/j.jhydrol.2004.12.010
- Budyko, M. I. (1974). Climate and Life. Academic Press.
- 607 Caldwell, P. V., Sun, G., McNulty, S. G., Cohen, E. C., & Moore Myers, J. A. (2012). Impacts of
- impervious cover, water withdrawals, and climate change on river flows in the
- conterminous US. *Hydrology and Earth System Sciences*, 16(8), 2839–2857.
- 610 https://doi.org/10.5194/hess-16-2839-2012
- 611 Cheng, L., Xu, Z., Wang, D., & Cai, X. (2011). Assessing interannual variability of
- evapotranspiration at the catchment scale using satellite-based evapotranspiration data sets.
- 613 *Water Resources Research*, 47, W09509. https://doi.org/10.1029/2011WR010636

- 614 Choudhury, B. J. (1999). Evaluation of an empirical equation for annual evaporation using field
- observations and results from a biophysical model. *Journal of Hydrology*, 216(1–2), 99–
- 616 110. https://doi.org/10.1016/S0022-1694(98)00293-5
- 617 Chu, H., Wei, J., Qiu, J., Li, Q., & Wang, G. (2019). Identification of the impact of climate
- change and human activities on rainfall-runoff relationship variation in the Three-River
- Headwaters region. *Ecological Indicators*, *106*, 105516.
- https://doi.org/10.1016/j.ecolind.2019.105516
- DeLucia, E. H., Chen, S., Guan, K., Peng, B., Li, Y., Gomez-Casanovas, N., Kantola, I. B.,
- Bernacchi, C. J., Huang, Y., Long, S. P., & Ort, D. R. (2019). Are we approaching a water
- ceiling to maize yields in the United States? *Ecosphere*, 10(6).
- 624 https://doi.org/10.1002/ecs2.2773
- Dewitz, J., & U.S. Geological Survey. (2021). National Land Cover Database (NLCD) 2019
- 626 Products (ver. 2.0, June 2021): U.S. Geological Survey data release.
- 627 https://doi.org/10.5066/P9KZCM54
- Dev, P., & Mishra, A. (2017). Separating the impacts of climate change and human activities on
- streamflow: A review of methodologies and critical assumptions. *Journal of Hydrology*,
- 630 548, 278–290. https://doi.org/10.1016/j.jhydrol.2017.03.014
- Diem, J. E., Hill, T. C., & Milligan, R. A. (2018). Diverse multi-decadal changes in streamflow
- within a rapidly urbanizing region. *Journal of Hydrology*, 556, 61–71.
- https://doi.org/10.1016/j.jhydrol.2017.10.026
- Dieter, C., Linsey, K. S., Caldwell, R. R., Harris, M. A., Ivahnenko, T. I., Lovelace, J. K.,
- Maupin, M. A., & Barber, N. L. (2018). Estimated Use of Water in the United States

- 636 County-Level Data for 2015 (ver. 2.0, June 2018): U.S. Geological Survey data release.
- 637 https://doi.org/10.5066/F7TB15V5
- Donohue, R. J., Roderick, M. L., & McVicar, T. R. (2012). Roots, storms and soil pores:
- Incorporating key ecohydrological processes into Budyko's hydrological model. *Journal of*
- 640 *Hydrology*, 436–437, 35–50. https://doi.org/10.1016/j.jhydrol.2012.02.033
- Du, C., Sun, F., Yu, J., Liu, X., & Chen, Y. (2016). New interpretation of the role of water
- balance in an extended Budyko hypothesis in arid regions. *Hydrology and Earth System*
- *Sciences*, 20(1), 393–409. https://doi.org/10.5194/hess-20-393-2016
- 644 Du, J., Qian, L., Rui, H., Zuo, T., Zheng, D., Xu, Y., & Xu, C. Y. (2012). Assessing the effects
- of urbanization on annual runoff and flood events using an integrated hydrological
- modeling system for Qinhuai River basin, China. *Journal of Hydrology*, 464–465, 127–139.
- https://doi.org/10.1016/j.jhydrol.2012.06.057
- Dudley, R. W., Hirsch, R. M., Archfield, S. A., Blum, A. G., & Renard, B. (2020). Low
- streamflow trends at human-impacted and reference basins in the United States. *Journal of*
- 650 *Hydrology*, 580, 124254. https://doi.org/10.1016/j.jhydrol.2019.124254
- Easterling, D. R., Arnold, J. R., Knutson, T., Kunkel, K. E., LeGrande, A. N., Leung, L. R.,
- Vose, R. S., Waliser, D. E., & Wehner, M. F. (2017). Ch. 7: Precipitation Change in the
- 653 United States. Climate Science Special Report: Fourth National Climate Assessment,
- 654 *Volume I.* https://doi.org/10.7930/J0H993CC
- Falcone, J. A. (2011). GAGES-II: Geospatial Attributes of Gages for Evaluating Streamflow
- 656 *metadata*. Available online at http://water.usgs.gov/GIS/metadata/usgswrd/
- 657 XML/gagesII Sept2011.xml

Falcone, J. A., Carlisle, D. M., Wolock, D. M., & Meador, M. R. (2010). GAGES: A stream 658 gage database for evaluating natural and altered flow conditions in the conterminous United 659 660 States. Ecology, 91(2), 621–621. https://doi.org/10.1890/09-0889.1 661 Frans, C., Istanbulluoglu, E., Mishra, V., Munoz-Arriola, F., & Lettenmaier, D. P. (2013). Are climatic or land cover changes the dominant cause of runoff trends in the Upper Mississippi 662 663 River Basin? Geophysical Research Letters, 40(6), 1104–1110. https://doi.org/10.1002/grl.50262 664 665 Fu, B. P. (1981). On the calculation of the evaporation from land surface. *Chinese Journal of* Atmospheric Sciences, 5(1), 23–31. https://doi.org/10.3878/j.issn.1006-9895.1981.01.03 666 667 Giri, S., Arbab, N. N., & Lathrop, R. G. (2019). Assessing the potential impacts of climate and land use change on water fluxes and sediment transport in a loosely coupled system. 668 Journal of Hydrology, 577, 123955. https://doi.org/10.1016/j.jhydrol.2019.123955 669 670 Greve, P., Burek, P., & Wada, Y. (2020). Using the Budyko Framework for Calibrating a Global Hydrological Model. Water Resources Research, 56(6), e2019WR026280. 671 https://doi.org/10.1029/2019WR026280 672 Greve, P., Gudmundsson, L., Orlowsky, B., & Seneviratne, S. I. (2015). Introducing a 673 probabilistic Budyko framework. Geophysical Research Letters, 42(7), 2261–2269. 674 675 https://doi.org/10.1002/2015GL063449 Guillén, L. A., Fernández, R., Gaertner, B., & Zégre, N. P. (2021). Climate and Landscape 676 Controls on the Water Balance in Temperate Forest Ecosystems: Testing Large Scale 677 Controls on Undisturbed Catchments in the Central Appalachian Mountains of the US. 678 Water Resources Research, 57, e2021WR029673. https://doi.org/10.1029/2021WR029673 679

- 680 Gupta, S. C., Kessler, A. C., Brown, M. K., & Zvomuya, F. (2015). Climate and agricultural land
- use change impacts on streamflow in the upper midwestern United States. *Water Resources*
- 682 Research, 51(7), 5301–5317. https://doi.org/10.1002/2015WR017323
- Haddeland, I., Heinke, J., Biemans, H., Eisner, S., Flörke, M., Hanasaki, N., Konzmann, M.,
- Ludwig, F., Masaki, Y., Schewe, J., Stacke, T., Tessler, Z. D., Wada, Y., & Wisser, D.
- 685 (2014). Global water resources affected by human interventions and climate change.
- 686 Proceedings of the National Academy of Sciences of the United States of America, 111(9),
- 687 3251–3256. https://doi.org/10.1073/pnas.1222475110
- Haddeland, I., Lettenmaier, D. P., & Skaugen, T. (2006). Effects of irrigation on the water and
- energy balances of the Colorado and Mekong river basins. *Journal of Hydrology*, 324(1–4),
- 690 210–223. https://doi.org/10.1016/j.jhydrol.2005.09.028
- Homer, C., Dewitz, J., Jin, S., Xian, G., Costello, C., Danielson, P., Gass, L., Funk, M.,
- Wickham, J., Stehman, S., Auch, R., & Riitters, K. (2020). Conterminous United States
- land cover change patterns 2001–2016 from the 2016 National Land Cover Database.
- 694 *ISPRS Journal of Photogrammetry and Remote Sensing*, 162, 184–199.
- 695 https://doi.org/10.1016/j.isprsjprs.2020.02.019
- 696 Istanbulluoglu, E., Wang, T., Wright, O. M., & Lenters, J. D. (2012). Interpretation of hydrologic
- trends from a water balance perspective: The role of groundwater storage in the Budyko
- 698 hypothesis. *Water Resources Research*, 48(1), W00H16.
- 699 https://doi.org/10.1029/2010WR010100
- Konikow, L. F. (2013). Groundwater Depletion in the United States (1900-2008).
- 701 https://doi.org/10.3133/sir20135079

- Koppa, A., & Gebremichael, M. (2017). A Framework for Validation of Remotely Sensed
- Precipitation and Evapotranspiration Based on the Budyko Hypothesis. *Water Resources*
- 704 Research, 53(10), 8487–8499. https://doi.org/10.1002/2017WR020593
- Kundu, S., Khare, D., & Mondal, A. (2017). Past, present and future land use changes and their
- impact on water balance. *Journal of Environmental Management*, 197, 582–596.
- 707 https://doi.org/10.1016/j.jenvman.2017.04.018
- Lawler, J. J., Lewis, D. J., Nelson, E., Plantinga, A. J., Polasky, S., Withey, J. C., Helmers, D. P.,
- Martinuzzi, S., Penningtonh, D., & Radeloff, V. C. (2014). Projected land-use change
- impacts on ecosystem services in the United States. *Proceedings of the National Academy*
- of Sciences of the United States of America, 111(20), 7492–7497.
- 712 https://doi.org/10.1073/pnas.1405557111
- Li, C., Sun, G., Caldwell, P., Cohen, E., Fang, Y., Zhang, Y., Oudin, L., Sanchez, G., &
- Meentemeyer, R. (2020). Impacts of urbanization on watershed water balances across the
- conterminous United States. *Water Resources Research*, 56(7), 1–19.
- 716 https://doi.org/10.1029/2019WR026574
- 717 Li, D., Pan, M., Cong, Z., Zhang, L., & Wood, E. (2013). Vegetation control on water and
- energy balance within the Budyko framework. *Water Resources Research*, 49(2), 969–976.
- 719 https://doi.org/10.1002/wrcr.20107
- 720 Li, H., Shi, C., Zhang, Y., Ning, T., Sun, P., Liu, X., Ma, X., Liu, W., & Collins, A. L. (2020).
- Using the Budyko hypothesis for detecting and attributing changes in runoff to climate and
- vegetation change in the soft sandstone area of the middle Yellow River basin, China.

- *Science of the Total Environment*, 703, 135588.
- 724 https://doi.org/10.1016/j.scitotenv.2019.135588
- Li, S., Du, T., & Gippel, C. J. (2022). A Modified Fu (1981) Equation with a Time-varying
- Parameter that Improves Estimates of Inter-annual Variability in Catchment Water Balance.
- 727 Water Resources Management, 36(5), 1645–1659. https://doi.org/10.1007/s11269-021-
- 728 03057-1
- Li, X., Tian, H., Lu, C., & Pan, S. (2023). Four-century history of land transformation by humans
- in the United States (1630-2020): annual and 1gkm grid data for the HIStory of LAND
- changes (HISLAND-US). Earth System Science Data, 15(2), 1005–1035.
- 732 https://doi.org/10.5194/essd-15-1005-2023
- Li, Z., & Quiring, S. M. (2021a). Identifying the Dominant Drivers of Hydrological Change in
- the Contiguous United States. *Water Resources Research*, 57(5), e2021WR029738.
- 735 https://doi.org/10.1029/2021WR029738
- Li, Z., & Quiring, S. M. (2021b). Investigating spatial heterogeneity of the controls of surface
- water balance in the contiguous United States by considering anthropogenic factors. *Journal*
- 738 of Hydrology, 601, 126621. https://doi.org/10.1016/j.jhydrol.2021.126621
- T39 Lins, H. F. (2012). USGS Hydro-Climatic Data Network 2009 (HCDN-2009): U.S. Geological
- 740 *Survey Fact Sheet 2012–3047.* Available online at https://pubs.usgs.gov/fs/2012/3047/
- Liu, J., & You, Y. (2021). The Roles of Catchment Characteristics in Precipitation Partitioning
- 742 Within the Budyko Framework. *Journal of Geophysical Research: Atmospheres*, 126(16),
- 743 e2021JD035168. https://doi.org/10.1029/2021JD035168

- Lv, X., Zuo, Z., Ni, Y., Sun, J., & Wang, H. (2019). The effects of climate and catchment
- characteristic change on streamflow in a typical tributary of the Yellow River. *Scientific*
- 746 Reports, 9(1), 14535. https://doi.org/10.1038/s41598-019-51115-x
- Mishra, V., Cherkauer, K. A., Niyogi, D., Lei, M., Pijanowski, B. C., Ray, D. K., Bowling, L. C.,
- 48 & Yang, G. (2010). A regional scale assessment of land use/land cover and climatic
- changes on water and energy cycle in the upper Midwest United States. *International*
- Journal of Climatology, 30(13), 2025–2044. https://doi.org/10.1002/joc.2095
- O'Driscoll, M., Clinton, S., Jefferson, A., Manda, A., & McMillan, S. (2010). Urbanization
- effects on watershed hydrology and in-stream processes in the southern United States.
- 753 *Water*, 2(3), 605–648. https://doi.org/10.3390/w2030605
- Overpeck, J. T., & Udall, B. (2020). Climate change and the aridification of North America.
- Proceedings of the National Academy of Sciences of the United States of America, 117(21),
- 756 11856–11858. https://doi.org/10.1073/pnas.1916208117
- Padrón, R. S., Gudmundsson, L., Greve, P., & Seneviratne, S. I. (2017). Large-Scale Controls of
- the Surface Water Balance Over Land: Insights From a Systematic Review and Meta-
- 759 Analysis. *Water Resources Research*, *53*(11), 9659–9678.
- 760 https://doi.org/10.1002/2017WR021215
- Parajuli, P. B., Jayakody, P., Sassenrath, G. F., & Ouyang, Y. (2016). Assessing the impacts of
- climate change and tillage practices on stream flow, crop and sediment yields from the
- 763 Mississippi River Basin. *Agricultural Water Management*, 168, 112–124.
- 764 https://doi.org/10.1016/j.agwat.2016.02.005

- Peel, M. C., McMahon, T. A., & Finlayson, B. L. (2010). Vegetation impact on mean annual
- evapotranspiration at a global catchment scale. *Water Resources Research*, 46(9), W09508.
- 767 https://doi.org/10.1029/2009WR008233
- Pielke, R. A., Pitman, A., Niyogi, D., Mahmood, R., McAlpine, C., Hossain, F., Goldewijk, K.
- K., Nair, U., Betts, R., Fall, S., Reichstein, M., Kabat, P., & de Noblet, N. (2011). Land
- use/land cover changes and climate: Modeling analysis and observational evidence. *Wiley*
- 771 Interdisciplinary Reviews: Climate Change, 2(6), 828–850. https://doi.org/10.1002/wcc.144
- Pike, J. G. (1964). The estimation of Annual runoff from metereological data in a tropical
- climate. Journal of Hydrology, 2, 116–123. https://doi.org/10.1016/0022-1694(64)90022-8
- Qiu, H., Niu, J., & Phanikumar, M. S. (2019). Quantifying the space time variability of water
- balance components in an agricultural basin using a process-based hydrologic model and
- the Budyko framework. *Science of the Total Environment*, 676, 176–189.
- https://doi.org/10.1016/j.scitotenv.2019.04.147
- 778 Reaver, N. G. F., Kaplan, D. A., Klammler, H., & Jawitz, J. W. (2022). Theoretical and
- 779 empirical evidence against the Budyko catchment trajectory conjecture. *Hydrology and*
- 780 Earth System Sciences, 26(5), 1507–1525. https://doi.org/10.5194/hess-26-1507-2022
- Rogger, M., Agnoletti, M., Alaoui, A., Bathurst, J. C., Bodner, G., Borga, M., Chaplot, V.,
- Gallart, F., Glatzel, G., Hall, J., Holden, J., Holko, L., Horn, R., Kiss, A., Kohnová, S.,
- Leitinger, G., Lennartz, B., Parajka, J., Perdigão, R., ... Blöschl, G. (2017). Land use
- change impacts on floods at the catchment scale: Challenges and opportunities for future
- research. Water Resources Research, 53(7), 5209–5219.
- 786 https://doi.org/10.1002/2017WR020723

787 Rost, S., Gerten, D., Bondeau, A., Lucht, W., Rohwer, J., & Schaphoff, S. (2008). Agricultural 788 green and blue water consumption and its influence on the global water system. Water Resources Research, 44(9), W09405. https://doi.org/10.1029/2007WR006331 789 790 Schilling, K. E. (2016). Comment on "Climate and agricultural land use change impacts on streamflow in the upper midwestern United States" by Satish C. Gupta et al. Water 791 792 Resources Research, 52(7), 5694–5696. https://doi.org/10.1002/2015WR018482 Schilling, K. E., Jha, M. K., Zhang, Y. K., Gassman, P. W., & Wolter, C. F. (2008). Impact of 793 794 land use and land cover change on the water balance of a large agricultural watershed: Historical effects and future directions. Water Resources Research, 44(7), W00A09. 795 796 https://doi.org/10.1029/2007WR006644 797 Shao, Q., Traylen, A., & Zhang, L. (2012). Nonparametric method for estimating the effects of climatic and catchment characteristics on mean annual evapotranspiration. Water Resources 798 Research, 48(3), W03517. https://doi.org/10.1029/2010WR009610 799 800 Sinha, J., Jha, S., & Goyal, M. K. (2019). Influences of watershed characteristics on long-term annual and intra-annual water balances over India. Journal of Hydrology, 577, 123970. 801 https://doi.org/10.1016/j.jhydrol.2019.123970 802 803 Sohl, T., Reker, R., Bouchard, M., Sayler, K., Dornbierer, J., Wika, S., Quenzer, R., & Friesz, A. 804 (2016). Modeled historical land use and land cover for the conterminous United States. *Journal of Land Use Science*, 11(4), 476–499. 805 https://doi.org/10.1080/1747423X.2016.1147619 806

807 Szilagyi, J. (2018). Anthropogenic hydrological cycle disturbance at a regional scale: State-wide evapotranspiration trends (1979–2015) across Nebraska, USA. Journal of Hydrology, 557, 808 600–612. https://doi.org/10.1016/j.jhydrol.2017.12.062 809 810 Tan, X., Liu, S., Tian, Y., Zhou, Z., Wang, Y., Jiang, J., & Shi, H. (2022). Impacts of Climate Change and Land Use/Cover Change on Regional Hydrological Processes: Case of the 811 812 Guangdong-Hong Kong-Macao Greater Bay Area. Frontiers in Environmental Science, 9, 783324. https://doi.org/10.3389/fenvs.2021.783324 813 814 Turc, L. (1954). The water balance of soils: relationship between precipitations, evaporation and flow (in French: Le bilan d'eau des sols: relation entre les précipitations, l'évaporation et 815 816 l'écoulement). Annales Agronomiques, Série A, 5, 491–595. 817 Vora, A., & Singh, R. (2021). Satellite based Budyko framework reveals the human imprint on long-term surface water partitioning across India. Journal of Hydrology, 602, 126770. 818 819 https://doi.org/10.1016/j.jhydrol.2021.126770 820 Wagner, P. D., Bhallamudi, S. M., Narasimhan, B., Kantakumar, L. N., Sudheer, K. P., Kumar, S., Schneider, K., & Fiener, P. (2016). Dynamic integration of land use changes in a 821 hydrologic assessment of a rapidly developing Indian catchment. Science of the Total 822 Environment, 539, 153–164. https://doi.org/10.1016/j.scitotenv.2015.08.148 823 Wagner, P. D., Kumar, S., & Schneider, K. (2013). An assessment of land use change impacts on 824 825 the water resources of the Mula and Mutha Rivers catchment upstream of Pune, India. Hydrology and Earth System Sciences, 17(6), 2233–2246. https://doi.org/10.5194/hess-17-826 2233-2013 827

Wang, D., & Hejazi, M. (2011). Quantifying the relative contribution of the climate and direct 828 human impacts on mean annual streamflow in the contiguous United States. Water 829 Resources Research, 47(9), W00J12. https://doi.org/10.1029/2010WR010283 830 831 Wang, D., & Tang, Y. (2014). A one-parameter Budyko model for water balance captures 832 emergent behavior in darwinian hydrologic models. Geophysical Research Letters, 41(13), 833 4569–4577. https://doi.org/10.1002/2014GL060509 Wehner, M. F., Arnold, J. R., Knutson, T., Kunkel, K. E., & LeGrande, A. N. (2017). Ch. 8: 834 835 Droughts, Floods, and Wildfires. Climate Science Special Report: Fourth National Climate Assessment, Volume I. https://doi.org/10.7930/J0CJ8BNN 836 Wing, O. E. J., Bates, P. D., Smith, A. M., Sampson, C. C., Johnson, K. A., Fargione, J., & 837 838 Morefield, P. (2018). Estimates of present and future flood risk in the conterminous United States. Environmental Research Letters, 13(3), 034023. https://doi.org/10.1088/1748-839 9326/aaac65 840 Xu, X., Liu, W., Scanlon, B. R., Zhang, L., & Pan, M. (2013). Local and global factors 841 controlling water-energy balances within the Budyko framework. Geophysical Research 842 Letters, 40(23), 6123–6129. https://doi.org/10.1002/2013GL058324 843 Yang, H., Yang, D., Lei, Z., & Sun, F. (2008). New analytical derivation of the mean annual 844 845 water-energy balance equation. Water Resources Research, 44(3), W03410. https://doi.org/10.1029/2007WR006135 846 Zhang, L., Hickel, K., Dawes, W. R., Chiew, F. H. S., Western, A. W., & Briggs, P. R. (2004). A 847 rational function approach for estimating mean annual evapotranspiration. Water Resources 848 Research, 40(2), W02502. https://doi.org/10.1029/2003WR002710 849

| 850 | Zhang, S., Yang, H., Yang, D., & Jayawardena, A. W. (2016). Quantifying the effect of |
|-----|--|
| 851 | vegetation change on the regional water balance within the Budyko framework. |
| 852 | Geophysical Research Letters, 43(3), 1140–1148. https://doi.org/10.1002/2015GL066952 |
| 853 | Zhang, Y., Gentine, P., Luo, X., Lian, X., Liu, Y., Zhou, S., Michalak, A. M., Sun, W., Fisher, J. |
| 854 | B., Piao, S., & Keenan, T. F. (2022). Increasing sensitivity of dryland vegetation greenness |
| 855 | to precipitation due to rising atmospheric CO2. Nature Communications, 13(1). |
| 856 | https://doi.org/10.1038/s41467-022-32631-3 |
| 857 | Zhao, J., Huang, S., Huang, Q., Leng, G., Wang, H., & Li, P. (2020). Watershed water-energy |
| 858 | balance dynamics and their association with diverse influencing factors at multiple time |
| 859 | scales. Science of the Total Environment, 711, 135189. |
| 860 | https://doi.org/10.1016/j.scitotenv.2019.135189 |
| 861 | Zhou, G., Wei, X., Chen, X., Zhou, P., Liu, X., Xiao, Y., Sun, G., Scott, D. F., Zhou, S., Han, L. |
| 862 | & Su, Y. (2015). Global pattern for the effect of climate and land cover on water yield. |
| 863 | Nature Communications, 6, 5918. https://doi.org/10.1038/ncomms6918 |
| | |